PHYSICAL REVIEW B VOLUME 11, NUMBER 5 1 MARCH 1975

Quantum-resistance states of superconducting Pb films*

L. G. Hayler,† L. M. Geppert, J. T. Chen, and Y. W. Kim
Department of Physics, Wayne State University, Detroit, Michigan 48202
(Received 26 August 1974)

We found that the I-V curves of a Pb film in a parallel magnetic field may consist of several linear current branches, characterized by a set of quantized resistances proportional to $n - \alpha$, where n is an integer and α is a field-dependent constant parameter between 0 and 1/2. The film thickness t and the parallel magnetic field $H_{\|}$ required for observing these quantum-resistance states are $\xi < t < 3\xi$ and $H_{c2} < H_{\|} < H_{c3}$, respectively. A simple phenomenological model based on the assumption that the film has a superconducting-normal-superconducting layer structure has been presented with the interpretation of the quantum resistances in terms of the momentum quantization of bound quasiparticles. Our data indicate that if the interpretation based on the bound quasiparticles is correct, then the quantum resistances we have observed are those with $\hbar k_{ZF} \ll (2m\Delta)^{1/2}$, where k_{ZF} is the component of the Fermi momentum perpendicular to the film surface.

I. INTRODUCTION

The current-voltage (I-V) characteristics of certain superconducting samples, such as microbridges, whiskers, and films, often show step structures associated with sudden jumps of voltage across the sample.[1-5] Although these I-V steps appear to be similar in general, several different mechanisms[4-7] may be involved as the steps have been observed under various experimental conditions. Thus, the investigation of instabilities in current-carrying superconductors is of both theoretical and experimental interest at present.

For the microbridges, Fink[6] proposes that the I-V steps are due to the periodic spatial variation of normal and super transport currents in parallel. Lately, Skocpol, Beasley, and Tinkham[5] suggest that local quantum phase-slip centers are responsible for the sudden voltage jumps. For the films, Huebener and Gallus[4] show that the development of small voltages is associated with the creation of moving normal channels. The common feature of all these proposed mechanisms is that the voltage steps are simply due to the addition of independent voltage centers connected in series. Each voltage center is associated with the formation of a superconducting-normal (SN) phase boundary *perpendicular* to the current flow and *due to* the current flow [Fig. 1(a)].

Recently, we have reported yet another type of structure observed in the I-V characteristics of a superconducting film in a parallel magnetic field.[8] The characteristic features of these structures and the experimental conditions under which they are observed are quite different from the ones we mentioned earlier. For example, they are observed in a parallel magnetic field above H_{c2}, the perpendicular critical magnetic field of the film, and at all temperatures below the transition temperature T_c. These structures are in the form of linear current branches characterized by constant slope and quantized dynamic resistance. It is proposed[8,9] that these quantum-resistance current branches represent different conducting states of coherent quasiparticles. The quantization of resistances comes from the quantization of the momentum components transverse to the film surface and the NS phase boundary. In other words, the quantum-resistance states have their origin in the NS phase boundary *parallel to* the current flow [Fig. 1(b)], and the formation of the NS phase boundary is *due to* the external parallel magnetic field. This is in contrast with the other proposed mechanisms in which the NS phase boundary is assumed to be perpendicular to the current flow and to be the result of the current flow.

In this article, we present the results of an experimental investigation of these quantum-resistance states. Based on the assumption proposed earlier, we develop a simple model using a rectangular pair potential well to interpret the experimental results. In the region the model is most likely to be valid, the agreement between experiment and theory is quite satisfactory. As a further test of this model and also to see whether a similar phenomenon is observable in other superconducting systems, an extensive investigation has also been made on ISN, SNI, ISNSI, INSNI sandwiches, where I represents an insulator. The results are found generally to be the same as those for an S film in a parallel magnetic field except for some differences which can be explained by taking into account the proximity effect at the NS phase boundary. The results of the investigations on these sandwiches will be presented elsewhere when they are completed.

II. EXPERIMENTAL DETAILS

A. Sample

The samples we have studied were Pb films prepared by thermal evaporation onto room-temperature quartz or glass substrates in a vacuum better than 3×10^{-6} Torr. The purity of the Pb sources was 99.9999% (A. D. McKay, Inc.). The rate of evaporation (typically 30 Å/sec) and the thickness of the film (several thousand angstroms) were controlled and monitored by a commercially available quartz-crystal oscillator unit [Sloan Omni II with sensing-head model 103-752]. After the evaporation, the films were first allowed to cool off in vacuum and then taken outside of the evaporator to be coated with a thin insulating layer of Kodak Ortho Resist for protection. When not used for measurement, samples were stored in liquid nitrogen. For the samples which were properly protected, the experimental results were reproducible after several months of storage.

The samples which yielded good results had mean free paths which were slightly less than 10^3 Å. The transition temperatures T_c of our Pb films were all approximately 7.2 K. The sample geometry is shown in Fig. 1(c), where the four dots represent the indium solder blobs for connecting electrical leads.

B. Low-temperature apparatus

The details of the sample holder are shown in Fig. 2. The sample is mounted on a copper block and held in place by a thin layer of vacuum grease (Apiezon type N with good thermal properties). The complete sample block with heating coil and calibrated germanium-resistance thermometer is enclosed in a vacuum-tight copper can sealed with an indium O ring.

The can assembly is immersed in a liquid-helium cryostat. The cryostat and placement of the sample holder with respect to the cryostat and magnet are shown in Fig. 2(c). The sample holder and the tail section of the cryostat fit between the pole pieces of a magnet. This allows a rotation of the magnetic field from parallel to perpendicular, relative to the plane of the film.

Temperatures between 1.4 and 4.2 K can be obtained by pumping above the helium bath. For temperatures above 4.2 K it is necessary to evacuate the can and to heat the sample block by using the heater coil. The sample block is partially isolated thermally by the vacuum in the can and also by the stainless steel tube to which the sample block is attached. Thus by changing the heater current, a steady temperature can be reached at any value up to 12 K. Temperature is measured by a calibrated germanium-resistance thermometer (CryoCal, Inc.).

C. Current-voltage measurement

The usual four-terminal arrangement and a constant-current source are used to measure the I-V characteristics of the films. Thus, any sudden transition of the films appears as a voltage jump with constant current value. In many situations, a complete I-V curve contains structures and hysterises which lead to multiple stable currents at the same voltage and also multiple stable voltages at the same current. Therefore, a single sweep-up-and-down trace of the I-V characteristic curve is not sufficient to reveal all the step structures. A brief description of I-V tracing techniques used for several different cases is given below.

The I-V characteristics for two different magne-

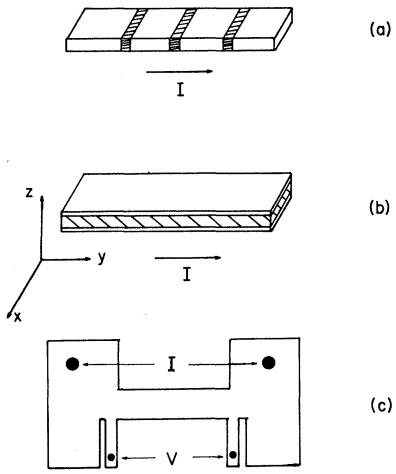

FIG. 1. Model for sample with NS phase boundaries (a) perpendicular and (b) parallel, to the current flow. (c) The sample geometry for this experiment.

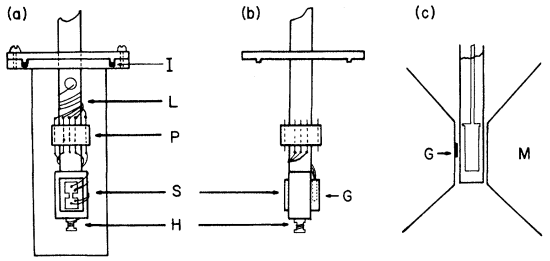

FIG. 2. (a) Sample holder with a vacuum can. I—indium O ring; L—leads; P—pins for electrical connection; S—substrate and sample; H—heater. (b) Side view of sample holder. G—germanium thermometer. (c) Relative position of sample with respect to the magnet poles which are rotatable about the vertical axis. M—magnet poles; G—gaussmeter probe.

tic fields are shown in Figs. 3 and 4. Each current branch has an upper and a lower critical voltage (or critical current). When the bias current is increased (or decreased) beyond these points, the film switches along a constant current line to the next stable point at higher (or lower) voltage. There are three classes of current branches, each of which requires a different tracing procedure. We call them: (a) the ascending step structure, (b) the inverted step structure, and (c) the "hidden-branch" structure.

For the ascending step structure, the current branches have upper critical currents that increase with increasing branch number n, so it is straightforward to trace out all the branches in increasing order. First, the bias current is slowly increased until the film switches to a higher branch, then it is varied down and up in that branch until the entire new branch is traced out, such as the $n=1$ branch shown in Fig. 3.

For the inverted step structure, the higher-n branches have upper critical currents which are less than those of lower n (see Fig. 4). In this case the bias current is first raised to a high value where the film is normal and then slowly decreased. The film does not make a smooth transition directly back to the zero-voltage superconducting state as the current is decreased. Instead, it jumps from one to another of a number of intermediate stable points along the returning section of the I-V curve. Starting at one of these points and increasing the bias current, a current branch is traced out. By repeating this procedure, each time starting with a different intermediate point, an I-V characteristic is traced out showing all of the intermediate current branches of the inverted-step-structure type.

The "hidden-branch" type of current structure has an upper critical current which is less than that of a branch with lower n while it also has a lower critical current which is greater than that of a higher-order branch (e.g., $n=1$ branch of Fig. 4). Therefore, it cannot be reached by the two methods described above. It is necessary to use a different technique to trace these branches. First, by varying the magnetic field, the relative amplitudes of the different current branches change. In general, the "hidden"-type current branches are found at lower magnetic fields while the ascending step structure is found at higher fields. At some convenient higher magnetic field, it is possible to bias by either of the first two methods to any of the current branches sought. After the film is biased to the desired branch, the magnetic field is adjusted to the correct value. When the required field is reached, the entire "hidden" branch can be traced out. We have used this technique to trace out the hidden branches at fields near H_{c2} and below (Fig. 5).

The magnetic field dependence can be studied by either (i) tracing out the entire I-V characteristic at each preset magnetic field (Figs. 3 and 4), or (ii) by biasing on a particular branch first and then varying the magnetic field. There is no noticeable

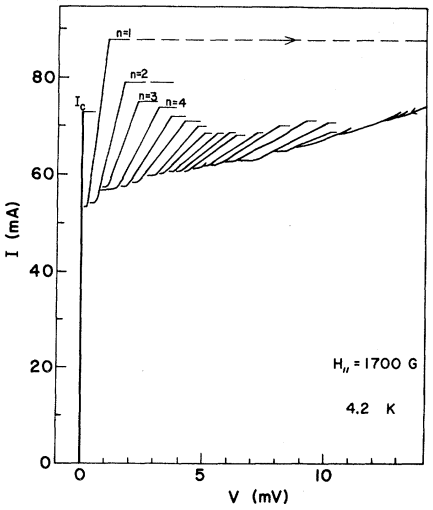

FIG. 3. $I-V$ characteristic of Pb film in field $H_{\parallel}$ = 1700 G showing several kinds of step structures. H_{c2} ~ 0.96 kG at 4.2 K.

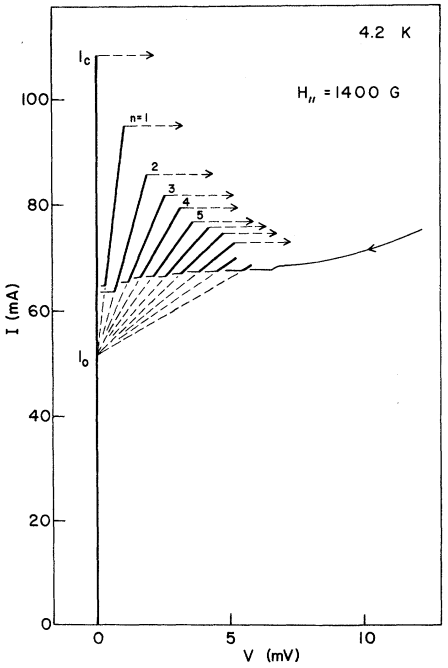

FIG. 4. $I-V$ characteristic of Pb film at 1400 G showing the inverted step structures.

difference in the I-V characteristics obtained by either method. The second method is especially convenient for studying changes in the shape, slope, and cutoff voltage of each branch. An example is shown in Fig. 6.

III. RESULTS AND INTERPRETATION

A. Current-voltage characteristics

If the film thickness is approximately $\xi < t < 3\xi$, where ξ is the coherence length, and when a parallel magnetic field $H_{\parallel}$ is chosen such that $H_{c2} \lesssim H_{\parallel} < H_{c3}$, where H_{c2} and H_{c3} are perpendicular and parallel critical fields, respectively, the I-V curves are as shown in Figs. 3 and 4. The sample for Figs. 3 and 4 has film thickness approximately 4000 Å and ξ about 1400 Å at 4.2 K.[10]

The main features of the I-V characteristics illustrated in Figs. 3 and 4 are as follows. There is a zero-voltage current, a normal-state current at higher voltage, and a series of additional current branches in between. Each of these intermediate current branches, called previously[8] intermediate quantum-resistance (IQR) states, has a nearly constant dynamic resistance $r_n = dV/dI$. The values of these dynamic resistances r_n are quantized in such a way that r_n increases with n. If these nearly linear current branches are extrapolated in straight lines back to zero voltage, the extrapolations I_{0n} all meet at a common intercept (labeled I_0 in Fig. 4). The current-voltage relations of these current branches can be described by the formula

$$I = I_{0n} + I_n = I_{0n} + V/r_n, \quad n = 1, 2, \ldots . \tag{1}$$

If the current in the nth branch is increased, eventually it reaches a critical value I_{cn}^{+} where this branch becomes unstable and the film switches to a stable branch at higher voltage. On the other hand, if the current in the nth branch is reduced, at some value I_{cn}^{-} the film switches to a stable branch at lower voltage. Since the intercept current is the same in both cases, these two critical currents can be written in the same form as

$$I_{cn}^{+} = I_{0n} + (I_n)_{\max} \quad \text{and} \quad I_{cn}^{-} = I_{0n} + (I_n)_{\min} . \tag{2}$$

Since the dynamic resistances r_n are nearly constant, Eq. (2) can also be written using critical voltages in place of the critical currents:

$$I_{cn}^{+} = I_{0n} + (V_n)_{\max}/r_n$$

and

$$I_{cn}^{-} = I_{0n} + (V_n)_{\min}/r_n . \tag{3}$$

So each quantum-resistance state is characterized by the parameters I_{0n} and r_n and the critical limits of each branch by either $(I_n)_{\max,\min}$ or $(V_n)_{\max,\min}$. In Sec. B we discuss a possible physical meaning for these parameters.

B. Interpretation

1. *Laminar structure*

Since the IQR states have been observed for $H_{c2} \lesssim H_{\parallel}$ and $\xi < t < 3\xi$, we assume that their origin lies in the laminar NS phase structure parallel to

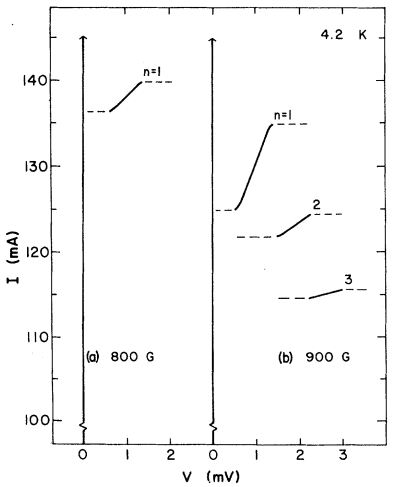

FIG. 5. $I-V$ characteristics of Pb film just below H_{c2}.

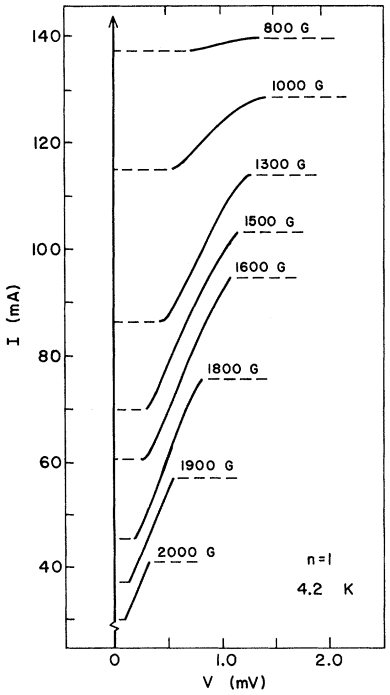

FIG. 6. The $n=1$ current branch characteristic for different parallel magnetic fields.

the film surface created by the parallel magnetic field. It is well known that a surface superconducting layer[11-17] can exist in a parallel magnetic field $H_{c3} > H_{\parallel} > H_{c2}$ when the film thickness t is greater than 1.8ξ. The two critical fields, H_{c2} and H_{c3}, depend on the Ginzburg-Landau parameter κ and the thermodynamic critical field H_c according to

$$H_{c2} = \sqrt{2}\ \kappa H_c \quad \text{and} \quad H_{c3} = 2.4\kappa H_c \ . \tag{4}$$

It should be noted that both type I ($\kappa < 0.71$) and type II ($\kappa > 0.71$) superconductors may have surface superconductivity if $\kappa > 0.42$.[13] Our Pb films which exhibit IQR states always have κ greater than this value. Although Pb is a type-I material, thin Pb films may behave as type II. In fact, our samples typically have $\kappa > 0.71$ determined experimentally by either using Eq. (4) for H_{c2} or the following formula:

$$\kappa = 0.96\,\lambda_L/\xi + 0.73\,\lambda_L/l \ , \tag{5}$$

where λ_L and l are the London penetration depth and the mean free path, respectively. In general, the κ values determined by these two methods agree within 30%. For example, the sample used for Figs. 3–11 has $\kappa = 1.3$ and 1.0 from Eq. (4) and Eq. (5), respectively. In Ref. 8, we have improperly classified our sample as type I. To explain our IQR states, we use a simple model in which a film in parallel field is assumed to have three layers, superconducting-normal-superconducting, with SNS phase boundaries parallel to the film surfaces.

2. *Excitation spectrum*

It has been shown[18-22] that for a superconductor in the intermediate state or a film with laminar SNS structure, there may exist bound quasiparticles with energy $E < \Delta$ in the normal region, where E is the bound quasiparticle energy measured relative to the Fermi surface and Δ is the maximum pair potential (order parameter). Kümmel[22] has made an extensive study of such bound states for the simple case where the pair potential has a step-type spatial distribution, i.e., $\Delta = 0$ in the normal region and $\Delta = \text{const}$ in the superconducting region. The bound states can be classified into two groups according to whether $\hbar k_{ZF}$ is greater or smaller than $\sqrt{2m\Delta}$, where k_{ZF} is the component of the Fermi vector in the direction perpendicular to the film surface which is in the X-Y plane. For $\hbar k_{ZF} \lesssim \sqrt{2m\Delta}$, i.e., those quasiparticles moving nearly parallel to the NS phase boundary, the momentum component transverse to the plane boundary is $k_{\perp n} = (\pi/d)n$.[22] However, our experimental results can be better understood if we assume that

$$k_{\perp n} = (\pi/d)(n - \alpha), \quad n = 1, 2, 3, \ldots \ , \tag{6}$$

where d is the normal layer thickness and α is a field-dependent constant, $0 < \alpha < \frac{1}{2}$. The quasiparticle energy corresponding to this momentum is

$$E_{\perp n} = (n - \alpha)^2 \hbar^2 \pi^2 / 2md^2 \ . \tag{7}$$

So the pair potential reflects the quasiparticles as an ordinary potential well.

For $\hbar k_{ZF} > \sqrt{2m\Delta}$, Andreev reflections[18] take place at the NS phase boundary. The momentum and the energy of the nth bound state are given as

$$k_{\perp n} = k_{ZF} \pm (\pi/d)(n - \alpha) \tag{8}$$

and

$$E_{\perp n} = (\hbar^2 k_{ZF}/m)(\pi/d)(n - \alpha) \ . \tag{9}$$

However, if the two S layers are thin (less than ξ), i.e., when $d \to t$, quasiparticles with $\hbar k_{ZF} > \sqrt{2m\Delta}$ will penetrate the S layers and be reflected from the outer film surfaces as though from ordinary infinite potential walls.

In any case, the quasiparticles with different k_x and k_y can be considered coherent if they have the same perpendicular component $k_{\perp n}$. In our model, we assume that each quantum-resistance state is the result of coherent conduction by quasiparticles with the same $k_{\perp n}$. We also simplify our model by considering only those quasiparticles with k_F nearly parallel to the phase boundary, i.e., those states described by Eqs. (6) and (7). Kümmel has also pointed out[22] that these states are not Andreev states but are the low-lying Generalized Andreev States which have properties similar to the bound states of ordinary reflection.

3. *Quantum resistances*

We assume that when the sample is biased on any of the quantum-resistance branches with I greater than I_0, there are two current components: I_{0n} and I_n. The I_{0n} component is equated with the time average of the Cooper-pair current in the superconducting layers. The other component, $I_n = V/r_n$, is equated with the quasiparticle current in the pair potential well of the normal layer. The zero-voltage current is conducted through the sample via the superconducting surface sheaths. In addition, we believe that resistanceless current flow also occurs in the normal layer since in this case the normal layer behaves as a gapless superconductor. This accounts for the fact that the zero-voltage critical current is larger than I_0 (Fig. 4).

To calculate the quasiparticle current, we assume that while the superconducting sheaths are

voltage biased, the current density j and the electric field $\mathcal{E}$, parallel to the SN phase boundary follow the relation

$$j = (n_q e^2 \tau/m)\mathcal{E} \ , \tag{10}$$

where e is the electronic charge, m is the quasiparticle mass, n_q is the quasiparticle density, and τ is the relaxation time for quasiparticles. A similar current-electric field relation has been proposed by Bardeen[23] for quasiparticle current flowing perpendicular to an NS phase boundary. The resistance of the normal layer when current is conducted by quasiparticles is then

$$r = \rho \frac{L}{wd} = \frac{\mathcal{E}}{j}\frac{L}{wd} = \frac{mL}{n_q e^2 wd\tau} \ , \tag{11}$$

where L, w, and d are, respectively, the length, width, and thickness of the normal layer and ρ is the electrical resistivity.

Thus the nature of the quasiparticle relaxation time τ determines the character of the resistance r. In a dirty film with short mean free path, the relaxation time depends on impurity scatterings. However, in a clean film quasiparticles can travel from one SN phase boundary to the other without impurity scattering. In this case we assume the relaxation time to be just the lifetime of a quasiparticle in the normal layer. This is just the transverse crossing time as a quasiparticle travels from one SN phase boundary to the other where it either decays in the superconductor as a Cooper pair and reflects a hole back into the normal layer or else is reflected back as in an ordinary potential well.

While the electric field accelerates quasiparticles parallel to the phase boundaries, it does not affect the transverse components $k_{\perp n}$ and $E_{\perp n}$. Thus the lifetime of a quasiparticle in crossing from one side of the normal layer to the other is independent of the electric field parallel to the phase boundaries. This requires that the mean free path of the film should not be too much smaller than d, the thickness of the normal layer. Then τ_n, the lifetime of a quasiparticle in the nth bound state, can be written

$$\tau = \tau_n = \frac{d}{v_{\perp n}} = \frac{md}{\hbar k_{\perp n}} = \frac{2md^2}{h(n-\alpha)} \ , \quad n = 1, 2, \ldots \ . \tag{12}$$

Combining Eqs. (11) and (12), we obtain

$$r_n = r_0(n-\alpha), \quad n = 1, 2, \ldots \ , \tag{13}$$

with

$$r_0 = hL/2n_q e^2 wd^3 \ .$$

The maximum voltage $(V_n)_{\max}$ and quasiparticle current $(I_n)_{\max}$ for each current branch can be obtained by considering the total energy E_n of a quasiparticle in an electric field. Relative to the Fermi level with terms of $k_{\parallel}^2$ neglected, we can write

$$E_n = \hbar k_F v_{dn} + \hbar^2 k_{\perp n}^2/2m \ , \tag{14}$$

where the drift velocity v_{dn} in an electric field $\mathcal{E}$ is

$$v_{dn} = \frac{e\mathcal{E}\tau_n}{m} = \frac{2eV_n d^2}{hL(n-\alpha)} \ , \quad n = 1, 2, \ldots \ . \tag{15}$$

For a bound state, the total energy of a quasiparticle is restricted so that $E_n \leq \Delta$. This requires that

$$\hbar k_F v_{dn} \leq \Delta - \hbar^2 k_{\perp n}^2/2m \tag{16}$$

or

$$(V_n)_{\max} = \frac{L\pi}{k_F e d^2}(n-\alpha)\left(\Delta - \frac{h^2}{8md^2}(n-\alpha)^2\right) \ . \tag{17}$$

The corresponding maximum current amplitude is then

$$(I_n)_{\max} = \frac{(V_n)_{\max}}{r_n} = \frac{n_q ewd}{\hbar k_F}\left(\Delta - \frac{h^2}{8md^2}(n-\alpha)^2\right) \ . \tag{18}$$

We have introduced quantum resistances and quasiparticle currents I_n in the nth quantum-resistance state. These involved voltages developed between the film ends. How do these voltages arise? A space and time dependence for the phase of the superconducting order parameter can develop along the SN boundaries. Kümmel[9] has offered an explanation of the voltage in terms of a time-dependent phase shift of the superconducting order parameter along the SN boundaries. He believes the decay of two excitations in the superconducting sheaths and scattering into a ground-state pair transfers their total momentum to the condensate. A superfluid vorticity may occur and a supercurrent is induced with a net gain in momentum. Thus a phase gradient appears between the film ends. The time change in the phase difference is equivalent to a voltage between the ends of the film. So the quasiparticle current, through the change in phase it causes along the SN boundaries between the film ends, can bias the superconducting layers at a nonzero voltage. For a constant quasiparticle current, a higher voltage difference develops along the film as the frequency of quasiparticle reflection at the SN boundary and interaction with the superconducting sheath increase. Therefore, $V_n \propto \nu_n \propto n$.

IV. COMPARISONS

In the preceding section, we have derived r_n and maximum V_n and I_n all in terms of the nor-

mal-layer thickness d. Experimentally, we cannot measure this thickness directly. However, it is reasonable to assume that the thickness d increases with applied magnetic field until it eventually reaches a limiting value of approximately the actual film thickness. Based on this assumption of field dependent d, we compare our experimental results with the theory as a function of magnetic field. We also show that one can deduce d as a function of $H_{\parallel}$ by fitting experimental r_n to Eq. (13). The d so deduced can be used to calculate other quantities, such as $(V_n)_{\max}$ and I_0 which can then be compared with the experimental data. In general, qualitative agreement can easily be obtained and in some cases agreement is even quantitative. The comparisons for each item are as follows.

A. Role of magnetic field

The experimental measurements indicate that it is quite critical for H to be parallel to the film surfaces. If the magnetic field is rotated from a parallel toward a perpendicular orientation, the current branches are quickly suppressed. In fact, the film can be accurately adjusted to a parallel orientation by observing the effect on the structures and their critical currents. Even a $\frac{1}{2}^\circ$ rotation away from parallel produces a noticeable drop in the critical current values and makes the structures very complicated, while a 10–15° rotation almost completely suppresses them. This is understandable in terms of a layer structure since flux penetration parallel to the SN boundaries tends to enhance the layer structure, but flux penetration perpendicular to the SN boundaries destroys the layer structure and allows fluxoids to be formed perpendicular to the film surfaces. On the other hand, the parallel magnetic field can be rotated in the plane of the film so that its orientation relative to the current is changed but there is no effect on the experimental measurements. This suggests that the importance of the magnetic field is to form the NS phase boundaries and to shape the potential well rather than to interact directly with the current.

Another indication of the importance of layers is that the field region $H_{c2} \lesssim H_{\parallel} \lesssim H_{c3}$ where structures are seen coincides with the region where laminas and surface superconductivity are present. Near but slightly below H_{c2}, only one branch is detected [Fig. 5(a)]. With gradual increase in magnetic field, more states appear in proper order as shown in Fig. 5(b).

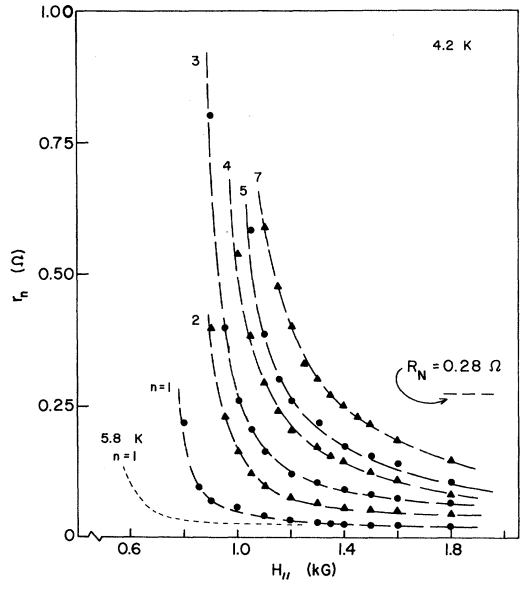

FIG. 7. Magnetic field dependence of the quantum resistances r_n at 4.2 K. R_N is the normal-state resistance of the film.

B. Behavior of r_n

As shown in Fig. 7, the quantum resistances exhibit a field dependence which qualitatively agrees with the prediction of our model. As $H_{\parallel}$ and thus d increase, the r_n's decrease rapidly to their respective limiting values. At a higher temperature, e.g., $T = 5.8$ K, IQR states are observed at lower field and with a smaller initial value of r_n (Fig. 8), due to a smaller H_{c2} and a larger $\xi(T)$. A larger coherence length means that a larger distance is required for the order parameter to vary from its maximum to zero, therefore the initial normal thickness d is larger. For comparison, we have plotted r_1 of 5.8 K together with r_1 of 4.2 K on the same scale in Fig. 7. We can see that their initial values at low field are different, but they approach to the same limiting value because of the same final d. The fact that the limiting values of r_n are independent of temperature but are dependent

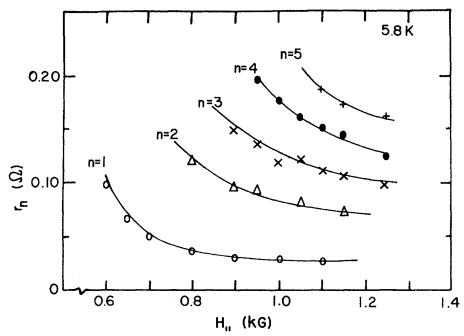

FIG. 8. Magnetic field dependence of the quantum resistances r_n at 5.8 K.

on d, makes it possible to check out the thickness dependence in a limited range. Measurements were taken on a set of three Pb films with thicknesses of 2000, 4000, and 6000 Å. The resistance spacings between levels, $r_2 - r_1 = \Delta r_{21}$, fell from 0.036 to 0.021 to 0.013 Ω as the film thickness increased. However, we do not stress the importance of this kind of measurement as a check of thickness dependence because the parameters, such as ξ and n_q, may differ from sample to sample. Particularly, if the sample does not satisfy the inequality $\xi < t < 3\xi$, the laminar structure may be quite different from a simple SNS type.

As shown in Fig. 7, r_n's at low fields may even be greater than the normal state resistance R_N of the film. This fact and the magnetic field dependence (r_n decreases with $H_\parallel$) cannot be expected from other models where partial resistances are due to the sectional normal regions created in series along the film length.

According to our simple model, $r_n = r_0(n - \alpha)$. But the experimental results for low fields show that r_n is not proportional to n (Fig. 9). This is expected because at low fields the potential well is not likely to be rectangular. In higher fields, however, the proportionality holds (above about 1300 G) and for this limiting case, the data agree with our theory in every respect. In this region, where we believe the normal lamina becomes limited by the film thickness, the pair potential well is most likely to have a rectangular form, and the bound states can be described by Eqs. (6) and (7).

C. $(V_n)_{\max}$

The maximum possible voltages for quantum-resistance states due to a rectangular pair potential well are given by Eq. (17). If d, Δ, and α as functions of magnetic field were known, the magnetic field dependence of $(V_n)_{\max}$ could be calculated from Eq. (17). Qualitatively speaking, in the field region where d and α do not vary significantly, $(V_n)_{\max}$ decreases rapidly with increasing field because of decreasing Δ. This behavior has been observed as shown in Figs. 10 and 11. For the magnetic field region $H_\parallel > 1.3$ kG, Fig. 9 shows that r_n vs n is nearly linear. This r_n vs n dependence together with the fact that all the current branches have the same intercept I_{0n} in this field region (Fig. 14) indicates that the rectangular pair potential well is a good approximation. We can then use Eqs. (13) and (17) to calculate the $(V_n)_{\max}$ for this magnetic field region and compare them with the experimental data.

Equation (13) and the data of r_n (e.g., Figs. 7–9) allow us to deduce d and α as functions of $H_\parallel$. The dimensions of the sample used for this calculation are $L = 0.25$ cm and $w = 0.032$ cm. In order to yield the correct value for r_0 we find that we have to use $n_q = 7.4 \times 10^{19}$ cm^{-3} which is only a small fraction of free electron density $n_e = 1.3 \times 10^{23}$ cm^{-3} for Pb. A similar calculation has also been done for the $T = 5.8$ K data. The required n_q is 4.5×10^{19} cm^{-3} and the corresponding d and α for both temperatures are shown in Fig. 12. We note that α is field dependent at $T = 4.2$ K, but not at

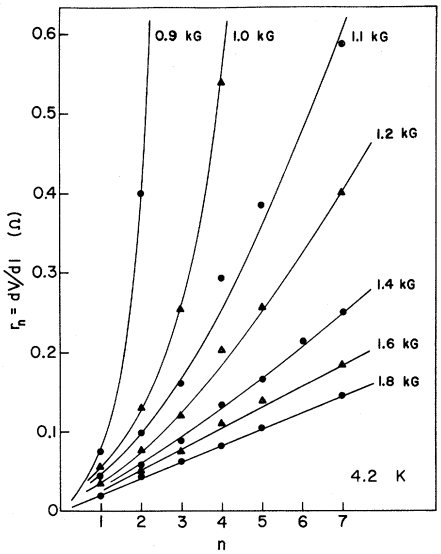

FIG. 9. Quantum resistances r_n vs quantum number n at different fields $H_\parallel$.

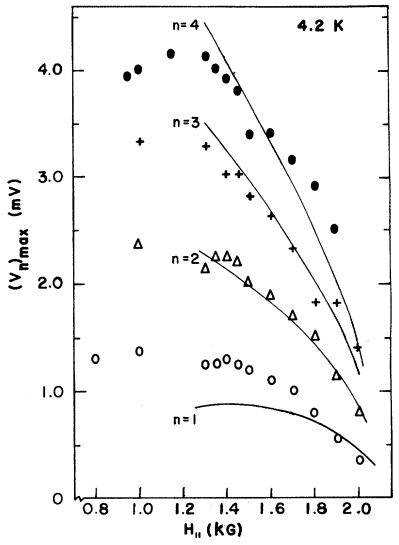

FIG. 10. Cutoff voltage $(V_n)_{\max}$ of the first several current branches at 4.2 K.

5.8 K where r_n also has only a weak field dependence (Fig. 8).

The value of the field dependent α has the same range $(0-\frac{1}{2})$ as α' for the generalized Andreev states discussed by Kümmel.[22] We also note that d initially increases rapidly and approaches a limiting value as $H_{\parallel}$ increases. Moreover, the initial d for $T=5.8$ K is larger than that for $T=4.2$ K.

The d and α so obtained can be used to calculate other quantities, such as $(V_n)_{\max}$, to see if they lead to consistent results. In order to compute $(V_n)_{\max}$, we need Δ. For that we use Eq. (17) and *only one* set of $(V_n)_{\max}$. The Δ deduced by using $(V_2)_{\max}$ is shown in Fig. 13. The Δ so obtained not only has a reasonable field dependence but also has the correct order of magnitude. (It is well known that for Pb, $\Delta=1.3$ meV for $H_{\parallel}=0$ at $T=4.2$ K.) The same Δ together with the d and α obtained from the r_n data lead to values of $(V_n)_{\max}$ for the other branches which are in good qualitative agreement with the experimental data as shown in Figs. 10 and 11. Even the quantitative agreement is within 30%. In these computations we have used $k_F=1.57\times10^8$ cm^{-1} according to the free electron model.

D. Number of branches

The total number $n_{\max}$ of IQR states increases with $H_{\parallel}$ at low fields because the bound-state energies decrease with increasing d [as predicted by Eq. (7)]. At the same time, Δ should not have a strong field dependence at low fields. At higher fields, d becomes nearly constant because it is limited by the film thickness. Thus, $n_{\max}$ decreases with increasing field as the depth of the pair-potential well becomes smaller. The total number of IQR branches has been observed to decrease at high field and also at higher temperature for the same reason. Not only does the qualitative dependence agree with the prediction, the actual number also agrees well with our model. For example, at $H_{\parallel}=1400$ G, d and Δ have been deduced from the experimental data to be 3400 Å and 0.3 meV, respectively. The value of $n_{\max}$ obtained by requiring that $E_{\perp n}\leq\Delta$ is 10. The agreement is excellent (Fig. 4).

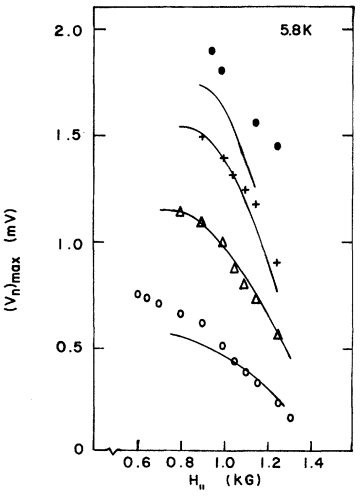

FIG. 11. Cutoff voltage of the first several current branches at 5.8 K.

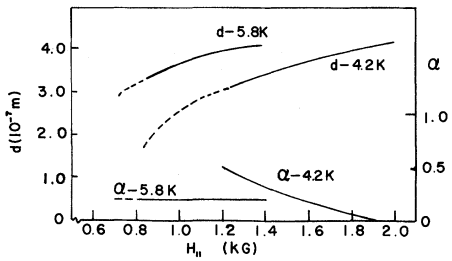

FIG. 12. Field dependences of the deduced normal-layer thickness d and the parameter α.

E. I_{0n} and I_0

As mentioned earlier, I_{0n} represents the current flowing through the superconducting surface sheaths (in the nonzero voltage state). For a rectangular pair potential well, the effective thickness of the S layers is the same for all states, therefore all I_{0n} should have the same value I_0. This is indeed the case (Fig. 14) for the field region $H_{\parallel}>1.3$ kG where r_n also can be described by $r_n=r_0(n-\alpha)$ (Fig. 9). For this region of magnetic field, where the rectangular well is probably a good assumption, we can approximate I_0 by $j_s w(t-d)$, where j_s is the supercurrent density and $t-d$ is the total thickness of the superconducting layers. Assuming $j_s\propto\Delta$,[24] we have calculated $\Delta(t-d)$ by

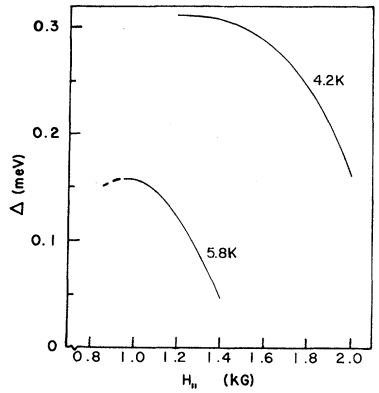

FIG. 13. Δ deduced from $(V_2)_{\max}$.

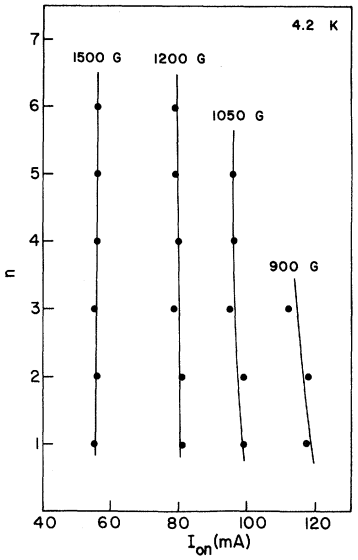

FIG. 14. Current intercepts for several different $H_{||}$.

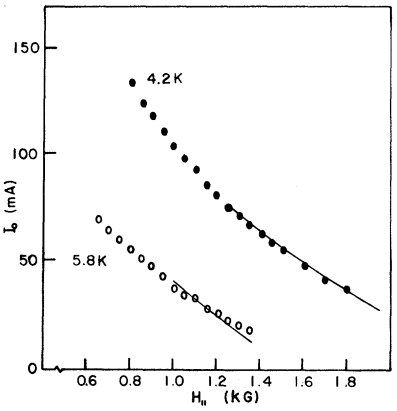

FIG. 15. The common current intercept I_0 vs $H_{||}$. Solid lines are theoretical curves (see explanation in text). For the magnetic field region where no solid lines are shown, not all the current branches have the same intercept I_0. The values of I_0 presented are those which are common to many but not all of the current branches.

using the values of Δ and d which were obtained previously from r_n and $(V_n)_{max}$ data. The results of the calculation, after normalization to fit one point, are shown as solid lines in Fig. 15. The agreement with the experimental points is indeed excellent for both $T = 4.2$ and 5.8 K. The total film thickness t required to give the fit shown in Fig. 15 is 5100 Å. The agreement of this value with the film thickness of 4000 Å estimated by use of a quartz oscillator during the evaporation is within 30%.

V. CONCLUSIONS

We have studied the properties of the quantum-resistance states of a superconducting film by assuming that they are due to the quantization of the transverse momentum component, $k_\perp = (\pi/d)(n - \alpha)$, of the bound quasiparticles. Based on the simple model of a rectangular pair potential well, we have derived expressions for several quantities associated with the quantum-resistance states. The agreement with the experimental results is quite satisfactory. Particularly in the magnetic field region where the two superconducting surfaces are thin, there is consistent agreement in every aspect. For example, for $H_{||} > 1.3$ kG, r_n is linear with respect to n, the I_{on} have the same value I_0, I_0 has the correct field dependence, and n_{max} agrees with the experiment. In addition, the calculated $(V_n)_{max}$, Δ, d, and α all have appropriate magnetic field dependences and correct magnitudes. It is remarkable that a parameter deduced from one experimentally measured quantity can be used to predict another with reasonable accuracy. If the quantum resistances we have observed are indeed due to the bound states, they correspond to the states with $\hbar k_{ZF} \ll \sqrt{2m\Delta}$.

We wish to point out that at present we have not understood the condition for calculating $(V_n)_{min}$. Also, there exists a quantitative discrepancy of 30% for $(V_n)_{max}$. We speculate that this may have something to do with the ground-state flow since the quasiparticle energy relative to the resting frame of reference is different from that relative to the frame of reference moving with the ground-state flow. If this is the case, Eq. (16) may have to be modified.

ACKNOWLEDGMENTS

We are grateful to Professor R. Kümmel for useful discussions and information on his work prior to its publication. We wish to thank Professor M. Tinkham and Dr. R. P. Huebener for sending us preprints.

*Work supported by the National Science Foundation through Grant No. GH-43837.

†Present address: Belfer Graduate School of Science, Yeshiva University, New York, N.Y. 10033.

[1]J. Meyer and G. V. Minnigerode, Phys. Lett. A 38, 529 (1972).

[2]W. W. Webb and R. T. Warburton, Phys. Rev. Lett. 20, 461 (1968).

[3]M. Sugahara, Phys. Rev. Lett. 29, 99 (1972); 29, 1318 (1972).
[4]R. P. Huebener and D. E. Gallus, Phys. Rev. B 7, 4089 (1973); Appl. Phys. Lett. 22, 597 (1973); Phys. Lett. A 44, 443 (1973).
[5]W. J. Skocpol, M. R. Beasley, and M. Tinkham, in *Proceedings of the International Conference on Magnetic Structures in Superconductors* (Argonne National Laboratory, Argonne, Ill., 1973); and report of work prior to publication.
[6]H. J. Fink, Phys. Lett. A 42, 465 (1973); A 43, 523 (1973); Phys. Status Solidi B 60, 843 (1973); H. J. Fink and R. S. Poulsen, Phys. Rev. Lett. 32, 762 (1974).
[7]John Clem, R. P. Huebener, and D. E. Gallus, J. Low Temp. Phys. 12, 449 (1973).
[8]J. T. Chen, L. G. Hayler, and Y. W. Kim, Phys. Rev. Lett. 30, 645 (1973).
[9]Reiner Kümmel, *Proceedings of the International Conference on Magnetic Structures in Superconductors* (Argonne National Laboratory, Argonne, Ill., 1973).
[10]ξ is calculated from $\xi = 0.74\ [\xi_p \xi_0 T_c/(T_c - T)]^{1/2}$ and $\xi_p^{-1} = \xi_0^{-1} + 0.75 l^{-1}$, where ξ_0 is the BCS coherence length and l is the mean free path.
[11]D. Saint-James and P. G. de Gennes, Phys. Lett. 7, 306 (1964).
[12]P. G. de Gennes, *Superconductivity of Metals and Alloys* (Benjamin, New York, 1966).
[13]A. C. Rose-Innes and E. H. Rhoderick, *Introduction to Superconductivity* (Pergamon, Oxford, England, 1969).
[14]J. D. Livingston and W. DeSorbo, in *Superconductivity*, edited by R. D. Parks (Marcel Dekker, New York, 1969), Chap. 21.
[15]H. J. Fink and R. D. Kessinger, Phys. Rev. 140, A1937 (1965).
[16]H. J. Fink, Phys. Rev. 177, 732 (1969).
[17]H. J. Fink, Phys. Rev. Lett. 14, 309 (1965).
[18]A. F. Andreev, Zh. Eksp. Teor. Fiz. 46, 1823 (1964); 49, 655 (1965) [Sov. Phys.—JETP 19, 1228 (1964); 22, 455 (1966)].
[19]G. A. Gogadze and I. O. Kulik, Zh. Eksp. Teor. Fiz. 60, 1819 (1971) [Sov. Phys.—JETP 33, 984 (1971)].
[20]C. Ishii, Prog. Theor. Phys. 44, 1525 (1970).
[21]John Bardeen and Jared L. Johnson, Phys. Rev. B 5, 72 (1972).
[22]Reiner Kümmel, Phys. Rev. B (to be published).
[23]J. Bardeen, in *Superconductivity*, edited by Frank Chilton (North-Holland, Amsterdam, 1971), pp. 114–123.
[24]John Bardeen, Rev. Mod. Phys. 34, 667 (1962).